Biological Psychiatry

Archival Report

Putamen Structure and Function in Familial Risk for Depression: A Multimodal Imaging Study

Ardesheer Talati, Milenna T. van Dijk, Lifang Pan, Xuejun Hao, Zhishun Wang, Marc Gameroff, Zhengchao Dong, Jürgen Kayser, Stewart Shankman, Priya J. Wickramaratne, Jonathan Posner, and Myrna M. Weissman

ABSTRACT

BACKGROUND: The putamen has been implicated in depressive disorders, but how its structure and function increase depression risk is not clearly understood. Here, we examined how putamen volume, neuronal density, and mood-modulated functional activity relate to family history and prospective course of depression.

METHODS: The study includes 115 second- and third-generation offspring at high or low risk for depression based on the presence or absence of major depressive disorder in the first generation. Offspring were followed longitudinally using semistructured clinical interviews blinded to their familial risk; putamen structure, neuronal integrity, and functional activation were indexed by structural magnetic resonance imaging (MRI), proton magnetic resonance spectroscopy (*N*-acetylaspartate/creatine ratio), and functional MRI activity modulated by valence and arousal components of a mood induction task, respectively.

RESULTS: After adjusting for covariates, the high-risk individuals had lower putamen volume (standardized betas, $\beta\text{-}_{left} = -0.17$, $\beta\text{-}_{right} = -0.15$, $ps = .002$), *N*-acetylaspartate/creatine ratio ($\beta\text{-}_{left} = -0.40$, $\beta\text{-}_{right} = -0.37$, $ps < .0001$), and activation modulated by valence ($\beta\text{-}_{left} = -0.22$, $\beta\text{-}_{right} = -0.27$, $ps < .05$) than low-risk individuals. Volume differences were greater at younger ages, and *N*-acetylaspartate/creatine ratio differences were greater at older ages. Lower putamen volume also predicted major depressive disorder episodes up to 8 years after the scan ($\beta\text{-}_{left} = -0.72$, $p = .013$; $\beta\text{-}_{right} = -0.83$, $p = .037$). Magnetic resonance spectroscopy and task functional MRI measures were modestly correlated ($0.27 \leq r \leq 0.33$).

CONCLUSIONS: Findings demonstrate abnormalities in putamen structure and function in individuals at high risk for major depressive disorder. Future studies should focus on this region as a potential biomarker for depressive illness, noting meanwhile that differences attributable to family history may peak at different ages based on which MRI modality is being used to assay them.

https://doi.org/10.1016/j.biopsych.2022.06.035

Major depressive disorder (MDD) is a chronic psychiatric disorder that is associated with significant clinical and functional impairment and increased mortality through both suicide and exacerbation of general medical conditions (1,2). MDD often runs in families, and offspring of parents with MDD have a 2- to 4-fold increased risk for developing depressive disorders themselves (3,4). The neurobiological mechanisms underlying this transmission, however, are not fully understood.

The putamen has increasingly emerged as a potential node in depression. Long recognized for its role in motor control and movement disorders, the putamen is part of the striatum and the cortico-striatal-thalamic circuits that govern reward learning and motivation—processes often compromised in depressed states (5). Several neuroimaging [including meta-analyses (6,7)] and postmortem morphometry (8) studies have documented smaller putamen volumes in patients with MDD; lower volumes have also been associated with anhedonia, a transdiagnostic marker linked to depression (9). In addition to structural differences, individuals with MDD show disruptions in putamen amplitude of low-frequency fluctuation at rest (10) and greater task activation in response to negative, relative to positive, stimuli (11).

While directly comparing individuals with and without MDD can identify brain regions of interest (ROIs), such regions could theoretically reflect predisposing mechanisms for, or sequelae of, the disorder. To better disentangle these mechanisms, Pagliacco *et al.* (12) used a high-risk design, examining brain volumes of 11,876 children at ages 9 to 10 years from the ABCD (Adolescent Brain Cognitive Development) cohort as a function of their parental depression history. They found that children who had one or more (vs. no) parents reporting a depressive disorder had significantly smaller putamen volumes, particularly in the right hemisphere, regardless of the offspring's own symptoms. These differences were observed in both a discovery and a replication subsample, with no other brain regions meeting these criteria.

SEE COMMENTARY ON PAGE e49

 ISSN: 0006-3223

This literature prompts 2 questions. First, because the studies mentioned previously have largely focused on single brain modalities, opportunities to build across units of analysis—a tenet of the National Institute of Mental Health's Research Domain Criteria approach (13,14)—have been limited. Different neuroimaging modalities provide complementary information about the brain's organization (15), and integrating across modalities may help better understand structure-function relationships and increase sensitivity/specificity for diagnostic prediction. Second, the long-term implications following emergence of putamen anomalies remain unclear without longitudinal follow-up (the ABCD study sample was preadolescent and has not traversed through the age of risk for MDD or other mood disorders). Whether these relationships are constant across ages is also unclear because prior studies have largely focused on a limited age range of participants.

In this study, we examined putamen structure and function in a 3-generation family study where second- and third-generation offspring were defined as at high or low risk for depression based on the presence or absence, respectively, of MDD in the first generation (16–18). The study began in 1982, and offspring have since been followed through multiple study waves (up to 38 years in the second generation) using blinded clinical interviews and multimodal brain scans. We have shown that the offspring of depressed parents (high-risk group) themselves have higher rates of depressive and anxiety disorders (17,18) and that offspring with 2 prior affected generations are at the greatest risk (19,20), demonstrating that the clinical risk is transmitted across generations.

Here, we harnessed this design to test biological risks. Specifically, we tested whether family history of depression would be associated with the following putamen markers: 1) volume (using high-resolution structural magnetic resonance imaging [MRI]); 2) neuronal integrity [*N*-acetylaspartate (NAA), a magnetic resonance spectroscopy (MRS)–derived marker of primarily neuronal origin, a decrease in which is interpreted as reduced neuronal viability (21)]; and 3) modulation of putamen activity by participants' valence and arousal ratings during a mood induction task (functional MRI [fMRI]). We tested these measures, collected during the same scan session, independently first, and then we tested the degree to which they are related. Finally, we examined whether these putamen markers would predict MDD up to 8 years postscan. We recognize that while such a region-of-interest focus may limit consideration of other depression-related (e.g., limbic) circuits, it allows us to interrogate multiple modalities and longitudinal psychiatric phenotypes within a single analytic framework and with fewer constraints imposed by multiple comparisons.

METHODS AND MATERIALS

Description of Cohort

The study began in 1982 with the recruitment of 2 groups of first-generation (G1) probands. The first group was recruited from outpatient clinics and included probands with moderate-to-severely impairing MDD and no lifetime history of psychotic, antisocial personality, bipolar, or primary substance use disorders (16–18). The second group included probands without depression who were selected from an epidemiological sample in the same community and who had no lifetime history of psychiatric illness as confirmed through several interviews. The second-generation (G2) and third-generation (G3) offspring of probands with MDD constitute the high-risk group and those of probands without MDD constitute the low-risk group. There have been 7 full waves to the study: years 0 (baseline), 2, 10, 20, 25, 30, and 38 (excluding a 40-year assessment recently completed in a partial sample to test health effects of the COVID-19 pandemic). G2 participants entered the study at year 0 or 2, whereas G3 participants entered at year 10 or 20 because they became eligible at age 6. Each interview assessed the period from the preceding interview; thus, the total follow-up window is cumulative until age at last interview. The design has been detailed elsewhere (16–18). Informed consent was obtained from adults for themselves and for their minor children; verbal assent was also obtained from minors. All procedures were approved by the New York State Psychiatric Institute's Institutional Review Board.

Clinical interviews were conducted at each wave by a trained mental health professional using the semistructured Schedule for Affective Disorders and Schizophrenia, lifetime version (22) [or the child/adolescent version for participants 6–17 years of age (23)]. Each family member was interviewed blinded to the clinical status of other family members. Interviewer training and reliability ranged from good to excellent, as documented elsewhere (17,18,20). Final diagnoses were confirmed by an M.D. or a Ph.D. clinician using the best-estimate procedure (24).

The primary analytical sample includes the 115 G2 and G3 participants who underwent an MRI scan and completed a diagnostic interview at year 30; 98 (85%) were reinterviewed approximately 8 years later. We have previously shown that individuals who completed the 38-year assessment did not differ significantly from those who did not on key clinical or demographic characteristics (25).

Neuroimaging Data Collection and Processing

Anatomical MRI. Images were acquired at New York State Psychiatric Institute using a GE Signa-3T scanner (GE Healthcare) with an 8-channel, phased array head coil using 3D fast spoiled gradient recall sequence (repetition time [TR]: 4.7 ms, echo time: 1.3 ms, flip angle: 110°, bandwidth: 41.67 MHz, field of view (FOV): 25 × 25 cm, array coil spatial sensitivity encoding (ASSET) factor: 2, slice thickness: 1.0 mm, matrix: 256 × 256, 128 slices, voxel dimension: 0.98 × 0.98 × 1.0 mm, 1 excitation per image × 2). Cortical and subcortical parcellations of the structural MRI scans were performed with FreeSurfer software version 5.3 (http://freesurfer.net), and these parcellations were used for individualized putamen regions.

Task-Based fMRI: Imaging. Functional images were acquired with echo-planar imaging sequence (TR = 2800 ms, echo time = 25 ms, flip angle = 90°, single excitation per image, 3-mm thickness, 0.5-mm gap, FOV 24 × 24 cm, 64 × 64 matrix, 43 slices, 189 TRs per run, voxel size 3.75 × 3.75 × 3.5 mm^3). Two runs were conducted per participant.

Task-Based fMRI: Mood Task. We used a mood induction task (26) in which participants were instructed as follows:

"You will be shown sentences that describe certain emotions. Try to think about what the emotion feels like." Each trial lasted 35 seconds and consisted of the following 3 components: 1) an emotional sentence (20 seconds); 2) ratings on arousal and valence dimensions (12 seconds); and 3) center crosshair (3 seconds). Ratings were presented as Likert-type scales for arousal (from −4 [low] to 4 [high]) and valence (from −4 [unpleasant] to 4 [pleasant]). Participants responded using a scanner-compatible computer mouse. The first rating bar (arousal) disappeared if no input was provided after 6 seconds, and the second rating bar (valence) appeared immediately after the first rating bar if there was an answer or if the response window timed out. Practice trials with different stimuli were provided.

Task-Based fMRI: Preprocessing of Functional Imaging Data. We used SPM8 (http://www.fil.ion.ucl.ac.uk/spm/) to preprocess the functional imaging data. The preprocessing procedure included the following steps: 1) slice-timing and motion correction; 2) spatial normalization to the standard Montreal Neurological Institute (MNI) template using a hybrid algorithm of affine transform and nonlinear warping; 3) normalization of each participant's structural image to the template; these person-specific warping parameters were then used to normalize the functional images to the same template; 4) reformatting of the normalized functional images to 3 × 3 × 3 mm voxels; and 5) Gaussian spatial filtering with a full width at half maximum of 8 mm. A discrete cosine transform-based high-pass filter with a basis function length of 128 seconds was also used to remove low-frequency noise, such as scanner drift, from the baseline image intensity.

Task-Based fMRI: Individual-Level Data Analysis for Detecting Whole-Brain Arousal- and Valence-Related Activity. We used SPM8 software to analyze the functional imaging data at the individual level (first-level analysis) to detect task-related activity within each individual participant. Using the general linear model as implemented in SPM8, we modeled data for each participant with 4 independent functions and a constant for each run. The first 2 independent functions corresponded to the 2 events (stimulation/presentation of emotional words and participants' ratings) recorded in the task, each of which was generated by convolving a canonical hemodynamic response function with a boxcar function derived from the onsets and durations of each of the events. The second 2 independent functions were generated by a separate amplitude modulation of the emotional stimulation function with each of the rating scores, the arousal score and the valence score. The model was estimated using the restricted maximum likelihood algorithm; task-related T-contrast images were then generated using SPM8, as also described previously (26).

Task-Based fMRI: ROI Analysis of Arousal- and Valence-Related Activity. To conduct the analysis of arousal- and valence-related activity based on ROI, we segmented high-resolution anatomical image (T1-weighted) into cortical and subcortical regions using FreeSurfer version 5.3. To apply participant-specific putamen ROIs generated from individual FreeSurfer subcortical segmentation (aseg.mgz file) to the functional contrast images (generated from the standard general linear model–based first-level analyses and described previously), we further used SPM12 to realign the functional contrast images (in MNI space) to the FreeSurfer subcortical segmentation image space (aseg.mgz) within each participant. Realignment was implemented by linearly coregistering the functional mean image (on the same MNI space as the contrast images) to the FreeSurfer intensity image space (brain.mgz), which was on the same space as the corresponding segmentation image (aseg.mgz), and then writing coregistration parameters back to the functional contrast images (summarized in Figure S1). We used these segmentations as ROIs to generate averaged activations from the arousal and valence contrast images.

Proton MRS: Acquisition. We acquired anatomical localizer images in the same slice locations as the multiplanar chemical shift imaging data. Scanning parameters were as follows: FOV = 24 × 24 cm^2, slice thickness = 10.0 mm, number of slices = 6, slice spacing = 2.0 mm, TR = 300 ms, echo time = 9 ms, acquisition matrix = 256 × 128 zero-padded to 256 × 256, effective in-plane resolution = 0.9375 × 0.9375 mm^2, slice orientation = oblique slices parallel to the anterior commissure-posterior commissure (AC/PC) line. We acquired the spectral data using 6 axial oblique slices parallel to the AC/PC line, with the second bottom-most slice containing the AC/PC line. Scanning parameters for the multiplanar chemical shift imaging data sequence were as follows (15): FOV = 24 cm, slice thickness = 10.0 mm, slice spacing = 2.0 mm, TR = 2300 ms, echo time = 144 ms, samples = 512 complex data points, number of phase encoding steps = 24 × 24, in-plane resolution = 10 × 10 mm^2. We suppressed water signal using the chemical shift selective imaging sequence and lipid signal by placing 8 angulated saturation bands around the brain.

Proton MRS: Processing. We processed MRS data using a processing pipeline (27,28), which is briefly summarized here. The k-space data were first 2D Fourier transformed after being spatially filtered by a Hamming window, together with residual water signal suppressed by a high-pass filter. Then the data at each voxel were 1D Fourier transformed to frequency domain, and its spectrum was spectrally fitted using a model-based approach to identify and integrate the spectrum for the singlets of NAA, creatine (Cr), and choline at each voxel. We performed partial volume correction on the MRS data to account for potential partial volume effects in the acquired data (28). The partial volume effects result from the following: 1) a large MRS voxel (1 × 1 × 1 cm^3) usually consists of varying proportions of gray matter, white matter, and cerebrospinal fluid; and 2) the limited number of k-space sampling points produces signal bleeding across voxels, termed a "point-spread-function" effect. We calculated the point-spread-function effect by simulating the MRS acquisition in k-space to generate a 24 × 24 complex array, which was then interpolated to 256 × 256 to match the high-resolution anatomical MR images. We also segmented the high-resolution MR images that were coregistered to the MRS slices into components of gray matter, white matter, and cerebrospinal fluid. We

convolved the components with the point-spread-function effect and used a linear regression model to compute the white matter and gray matter metabolite, respectively, inside each MRS voxel.

We focused on NAA, given its role as a marker of neuronal integrity, which was operationalized as a ratio of NAA to Cr (NAA/Cr), with Cr providing an internal reference. Cr reference did not vary significantly across high-risk (mean ± SD = 0.20 ± 0.09) and low-risk (mean ± SD = 0.16 ± 0.08) groups (p = .10; adjusted for sex, age, and receiver/transmitter gains). The normalization of MRS data into a template space was carried out using a 2-step procedure. First, the localizer image that was in ideal alignment with the multiplanar chemical shift imaging data was coregistered to the high-resolution anatomical image of the same participant using rigid body transformation. Second, the high-resolution anatomical image was normalized to the study template using standard procedure using a combined linear transformation and a nonlinear warping. The combined transformation of these 2 steps was then applied to the spectrally fitted data to generate results in the template space for group analyses.

Statistical Analysis

Analyses were conducted using SAS software (version 9.4). For demographic variables, comparisons were conducted using χ^2 tests for categorical variables and two-tailed t tests for continuous variables. To test associations between family history and each putamen marker, we used linear regressions with the putamen marker as the continuous outcome, familial risk (high = 1, low = 0) as the exposure, and age at time of scan and sex as covariates. For interpretability, we report standardized coefficients. When putamen volume was the outcome, analyses were further adjusted for total intracranial volume. To formally test for age interactions, risk-by-age terms were added to the models.

To test whether the putamen markers predicted depression up to 8 years later, we ran a generalized estimating equations model with the presence or absence of ≥1 MDD episode with onset date after the MRI scan as the outcome; putamen marker as the independent variable; and sex, age at scan, and the presence or absence of MDD prior to scan date as covariates. A link function was added to adjust for potential nonindependence of outcomes from related individuals.

RESULTS

Individuals at high risk for MDD had higher rates of lifetime MDD than those at low risk for MDD (54% vs. 21%); however, the groups did not vary by age, sex, education, income, or employment (Table 1).

Family History Predicts Putamen Volume, Neuronal Integrity, and Valence-Modulated Activity

After adjusting for sex, age, and (for volume outcomes) total intracranial volume, individuals at high risk compared with low risk had significantly lower volume in both hemispheres of the putamen (standardized betas: $\beta\text{-}_{left} = -0.17$, $\beta\text{-}_{right} = -0.15$, ps = .002); lower NAA/Cr ($\beta\text{-}_{left} = -0.40$, $\beta\text{-}_{right} = -0.37$, ps < .0001); and lower valence- (but not arousal-) modulated putamen activity ($\beta\text{-}_{left} = -0.21$, $\beta\text{-}_{right} = -0.25$, ps < .05) (Table 2, left).

To rule out the possibility that the putamen differences emerged because of having MDD, we repeated the above-mentioned analyses excluding any participant who had ever had MDD up to the time of the scan. As shown in the right panels of Table 2, associations between family history and putamen volume, NAA/Cr, and valence measures each remained statistically significant and with comparable effect sizes. They also remained significant after controlling for 1) any anxiety disorders by the time of scan (as these disorders were more common in the high-risk as compared with the low-risk group) (Table S1) and 2) putamen volume for the non–volume-based (i.e., the MRS and fMRI) outcomes (Table S2). A correlation matrix (Table S3) shows high coherence between left and right hemispheres within modalities ($0.82 \leq r\text{s} \leq 0.95$, ps < .0001). Across modalities, there was a small positive correlation between NAA/Cr- and valence-associated activation ($0.26 \leq r\text{s} \leq 0.33$, ps < .05), but there were no associations between any other combinations of modalities.

Given known changes in putamen structure with age (29,30), we examined whether associations between familial risk and putamen markers might also vary as a function of participant age. When risk-by-age interaction terms were added to each model shown in Table 2, interactions were significant for NAA/Cr (left putamen, p = .041), with a nonsignificant trend for volume (right putamen, p = .075; all other interaction, ps > .20). To understand the directions of the effects driving these interactions, we plotted putamen volume and NAA/Cr within each individual as a function of their age at scan (Figure 1). The plots illustrate that volume differences between high- and low-risk offspring are more prominent at younger ages (i.e., where the high- and low-risk lines are at their most divergent), while NAA/Cr differences are more prominent at older ages.

To operationalize these patterns further, we stratified the sample into individuals younger than 30 years (n = 63) versus individuals who were 30 years and older (n = 52) [we selected this cut-off because it is often used as a marker for early-onset depression, which is associated with greater genetic underpinnings and higher morbidity (31)]. Family history predicted right putamen volume only in individuals younger than 30 years ($\beta = -0.21$, p = .014; for those 30 years and older: $\beta = -0.07$, p = .53); conversely, family risk prediction of NAA/Cr was greater in individuals who were 30 years and older ($\beta\text{-}_{left} = -0.53$, p = .001; $\beta\text{-}_{right} = -0.47$, p = .004) than in individuals under 30 ($\beta\text{-}_{left} = -0.30$, p = .046; $\beta\text{-}_{right} = -0.30$, p = .047).

While the second-generation (G2) participants had only 1 prior generation, G3 participants could have a parent and/or a grandparent with MDD. As shown in Table S4, grandparental (G1 probands) and parental (G2) depression predicted G3 volume; however, only grandparental MDD predicted MRS and fMRI outcomes.

Prospective Analyses: Putamen Volume Predicts Depression Up to 8 Years Later

Finally, we explored whether the putamen differences predicted new episodes of MDD based on the 98 (85%) individuals who were clinically followed to approximately 8 years after the MRI scan (Table 3); demographic characteristics of

Table 1. Demographic and Clinical Characteristics

Characteristic	All Offspring, N = 115	Familial Risk Status		Group Comparison	
		High Risk, n = 63	Low Risk, n = 52	Statistics	p Value
Age, Years	32.3 (14.1) [10.7–59.1]	34.2 (14.4) [12.9–59.1]	30.0 (13.4) [10.7–56.2]	F = 1.17	.576
Lifetime MDD	–	–	–	χ^2 = 12.88	<.001[a]
Yes	45 (39.1%)	34 (54.0%)	11 (21.2%)	–	–
No	70 (60.9%)	29 (46.0%)	41 (78.9%)	–	–
Sex				χ^2 = 0.18	.672
Female	55 (47.8%)	29 (46.0%)	26 (50.0%)	–	–
Male	60 (52.2%)	34 (54.0%)	26 (50.0%)	–	–
Generation				χ^2 = 5.44	.020[b]
G2	49 (42.6%)	33 (52.4%)	16 (30.8%)	–	–
G3	66 (57.4%)	30 (47.6%)	36 (69.2%)	–	–
Education Level				χ^2 = 0.34[c]	.558
< High school diploma or less	60 (61.9%)	33 (64.7%)	27 (58.7%)	–	–
<4-year college	10 (10.3%)	6 (11.8%)	4 (8.7%)	–	–
Undergraduate degree	17 (17.5%)	6 (11.8%)	11 (23.9%)	–	–
Graduate degree	10 (10.3%)	6 (11.8%)	4 (8.7%)	–	–
Employment Status				χ^2 = 1.02	.313
Full-time employment	64 (66.0%)	36 (70.6%)	28 (60.9%)	–	–
Part-time or no employment	33 (34.0%)	15 (29.4%)	18 (39.1%)	–	–
Marital Status				χ^2 = 8.83	.032[b]
Single, never married	51 (52.6%)	24 (47.1%)	27 (58.7%)	–	–
Married, first marriage	31 (32.0%)	14 (27.5%)	17 (37.0%)	–	–
Separated or divorced	10 (10.3%)	8 (15.7%)	2 (4.4%)	–	–
Remarried	5 (5.1%)	5 (9.8%)	0 (0.0%)	–	–
Psychiatric History (Lifetime)					
Any psychotic disorder	1 (0.9%)	1 (1.6%)	0 (0.0%)	χ^2 = 0.83	.362
Bipolar disorder[d]	7 (6.1%)	6 (9.5%)	1 (1.9%)	χ^2 = 2.88	.090
Any anxiety disorder[e]	36 (31.3%)	27 (42.9%)	9 (17.3%)	χ^2 = 8.65	.003[f]
Any drug or alcohol use disorder	30 (26.1%)	18 (28.6%)	12 (23.1%)	χ^2 = 0.45	.504

MDD, major depressive disorder.
[a] $p < .001$.
[b] $p < .05$.
[c] Data were determined using the Kruskal-Wallis test.
[d] Includes bipolar I disorder, bipolar II disorder, cyclothymia, or bipolar disorder not otherwise specified.
[e] Includes panic disorder, social phobia, specific phobia, generalized anxiety disorder, separation anxiety disorder, obsessive-compulsive disorder, posttraumatic stress disorder, and anxiety disorder not otherwise specified.
[f] $p < .01$.

this subcohort are shown in Table S5. Of the 98 individuals, 27 (27.5%) had at least 1 MDD episode that started after the scan date; of these, 21 (78%) had 1 episode, 3 had 2 episodes, 2 had 3 episodes, and 1 had 4 episodes. Lower volume (β-$_{left}$ = −0.63, p = .022; β-$_{right}$ = −0.72, p = .071 [trend]) was associated with later MDD; these associations remained significant after adjusting for any mood disorder in the past (β-$_{left}$ = −0.73, p = .013; β-$_{right}$ = −0.82, p = .037). Lower arousal modulation also predicted future MDD (β-$_{left}$ = −0.62, p = .009).

When explored separately for individuals who were younger than 30 years (n = 52, of whom 19 [37%] had ≥1 major depressive episode post scan) versus those who were 30 years of age or older (n = 46, of whom 8 [17.4%] had an episode post scan), the association between lower volume and MDD up to 8 years later was observed only in the individuals under 30 (β-$_{left}$ = −0.9, p = .009; β-$_{right}$ = −1.2, p = .029); the full set of results is shown in Table S6.

DISCUSSION

Our findings support the putamen as a neural substrate in the transmission of MDD. We found that 1) having a family history of depression is associated with lower putamen volume, lower neuronal integrity, and diminished valence-modulation of putamen activity; 2) these associations are each independent of the participant's history of depression, supporting their roles as predisposing biomarkers; and 3) lower putamen volume is associated with future MDD episodes up to 8 years after the scan, even after adjusting for prior depression.

The putamen, through cortico-thalamo-striatal pathways, is known to modulate the experience of pleasure and reward. Lower putamen volumes are associated with greater anhedonia, and individuals with smaller putamen demonstrate blunted responses to positive feedback (9,32,33). A study comparing adults with and without MDD showed that in participants without depression, viewing facial expressions of

Table 2. Family History of Depression Predicts Putamen Structure and Function

Predictors		All Offspring, N = 115				Offspring With No MDD at Scan, n = 70			
		β[a]	t Value	p Value[b]	F Value (p Value)	β[a]	t Value	p Value	F Value (p Value)
Volume									
Left	Familial risk	−0.17	−2.65	.009[b]	34.99 (<.001)	−0.25	−3.22	.002[b]	24.05 (<.001)
	ICV	0.41	5.39	<.001[c]		0.47	4.83	<.001[c]	
	Age	−0.41	−6.31	<.001[c]		−0.39	−4.75	<.001[c]	
	Sex	0.15	2.01	.047[d]		0.07	0.79	.434	
Right	Familial risk	−0.15	−2.35	.020[d]	35.10 (<.001)	−0.26	−3.28	.002[b]	22.85 (<.001)
	ICV	0.38	4.94	<.001[c]		0.37	3.77	<.001[c]	
	Age	−0.44	−6.77	<.001[c]		−0.41	−4.92	<.001[c]	
	Sex	0.17	2.28	.025[d]		0.18	1.82	.073	
NAA/Cr									
Left	Familial risk	−0.40	−3.96	<.001[c]	8.69 (<.001)	−0.36	−2.72	.009[b]	3.71 (.018)
	Age	−0.24	−2.36	.021[d]		−0.26	−1.97	.054	
	Sex	−0.07	−0.71	.480		−0.01	−0.09	.926	
Right	Familial risk	−0.37	−3.60	.001[b]	6.86 (<.001)	−0.33	−2.48	.017[d]	2.59 (.064)
	Age	−0.20	−1.93	.057		−0.15	−1.12	.270	
	Sex	−0.07	−0.67	.507		−0.08	−0.57	.571	
fMRI Valence									
Left	Familial risk	−0.21	−1.98	.051	1.77 (.159)	−0.22	−1.63	.110	1.46 (.236)
	Age	−0.07	−0.63	.529		−0.19	−1.38	.173	
	Sex	−0.12	−1.13	.260		−0.06	−0.41	.682	
Right	Familial risk	−0.25	−2.37	.020[d]	2.32 (.081)	−0.28	−2.12	.039[d]	2.11 (.111)
	Age	−0.06	−0.55	.584		−0.19	−1.43	.157	
	Sex	−0.13	−1.20	.234		−0.06	−0.48	.630	
fMRI Arousal									
Left	Familial risk	0.00	−0.01	.993	0.50 (.686)	−0.10	−0.72	.477	0.69 (.559)
	Age	0.12	1.13	.263		0.09	0.64	.525	
	Sex	0.07	0.62	.536		0.15	1.09	.283	
Right	Familial risk	−0.05	−0.44	.664	1.50 (.221)	−0.12	−0.93	.356	1.24 (.304)
	Age	0.22	2.07	.041		0.22	1.64	.107	
	Sex	−0.01	−0.07	.941		0.04	0.29	.776	

fMRI, functional magnetic resonance imaging; ICV, intracranial volume; MDD, major depressive disorder; NAA/Cr, *N*-acetylaspartate/creatine ratio.
[a]Standardized beta.
[b]$p < .01$.
[c]$p < .001$.
[d]$p < .05$.

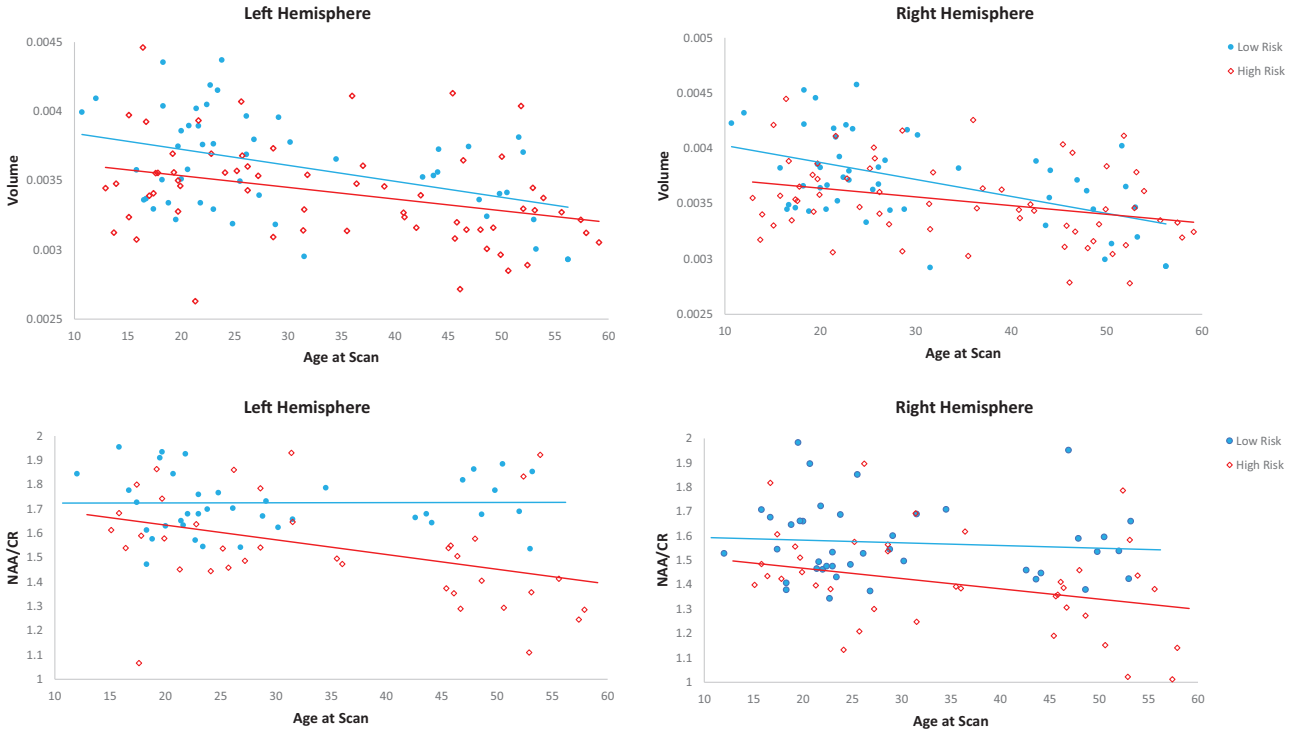

Figure 1. Individual-level data showing putamen volume and ratio of NAA to Cr (NAA/Cr) by age as a function of familial risk for depression. Plots show the distributions of putamen volume (top) and NAA/Cr (bottom) as a function of age for each individual in the study. Red and blue circles indicate individuals at high and low familial risk, respectively; red and blue lines represent the trend lines for these 2 groups. The figure illustrates the interaction between familial risk and putamen structure by age. For volume, there is an overall reduction of putamen volume with age; however, this reduction is greater at younger ages (illustrated by the greater divergence of the 2 lines at lower x-axis values). For NAA/Cr (lower panel), the opposite is noted, with risk differences emerging at later ages. Cr, creatine; NAA, *N*-acetylaspartate.

increasing happiness was associated with linear increases in putamen activation; in individuals with depression, facial expressions of increasing sadness were associated with increases in putamen activity (11). However, viewing of faces cannot separate whether neural responses are linked to stimulus valence (varying between pleasant and unpleasant) or stimulus arousal (varying between low and high levels of activation of the experienced feeling) (34). This is especially pertinent because previous studies have implicated the putamen in valence (35) and arousal (36) as well as in motor function and motivation. Using a mood induction task, we were able to distinguish between valence and arousal dimensions and vary the level of these dimensions to probe whether putamen blood oxygen level–dependent response was linearly correlated to these dimensions and differed by family risk status. We showed that the association of risk for depression and putamen activation is associated with differential valence, but not with arousal.

Within each modality, small effect sizes were observed for volumetric ($-0.15 \leq \beta \leq -0.17$) and fMRI ($-0.21 \leq \beta \leq -0.25$) outcomes, and moderate effects were observed for neuronal integrity ($-0.37 \leq \beta \leq -0.40$). Importantly, none of these associations abated when analysis was restricted to individuals with no history of MDD until the scan. Across modalities, we found modest associations between MRS (NAA/Cr) and fMRI (valence only) data ($0.26 \leq r \leq 0.33$), but not between other combinations of brain modalities. Other studies have similarly noted individual associations with disorders that do not stretch across different units of analysis (37–39). The tendency for variables to group within rather than across modalities may be exacerbated in psychopathological states where there is already disruption of normative physiological structure-function coupling [e.g., (40)]. Our findings also invite consideration of the age at which these modalities are assessed. Following adolescence, there is significant shrinking in putamen structure (29,30,41). Even when age is controlled for, the diminished overall structure at older ages may provide a floor that precludes detection of further risk-related changes. This is consistent with Figure 1, which shows both an overall reduction in putamen volume with increasing age and that the "delta" between the high- and low-risk offspring in putamen volumes diminishes with increasing age. In other words, putamen markers may be a poorer biomarker or predictive tool in older populations. In contrast, MRS-derived differences become prominent at later ages. Because the MRI modalities were collected concurrently, our data cannot speak to whether the volumetric abnormalities lead to NAA/Cr changes in subsequent years. However, the patterns clearly suggest that brain differences attributable to family history may peak at different ages based on which MRI modality is being used to

Table 3. Associations Between Putamen Markers and Major Depressive Disorder Up to 8 Years Later

		Controlling for Age and Sex			Controlling for Age, Sex, and MDD Until Time of Scan			Controlling for Age, Sex, Risk, and MDD Until Time of Scan		
Predictor		β	*z* Value	*p* Value	β	*z* Value	*p* Value	β	*z* Value	*p* Value
Volume										
Left	Volume	−0.63	−2.29	.022[a]	−0.72	−2.48	.013[a]	−0.62	−2.02	.043[a]
	Age	−1.09	−3.95	<.001[b]	−1.48	−6.04	<.001[b]	−1.45	−5.32	<.001[b]
	Sex	0.16	0.25	.802	0.18	0.29	.772	0.17	0.26	.798
	ICV	0.33	1.23	.218	0.35	1.21	.226	0.31	1.07	.287
	Add: MDD until scan	–	–	–	1.39	3.14	.002[c]	1.22	2.52	.012[a]
	Add: familial risk	–	–	–	–	–	–	0.67	1.56	.119
Right	Volume	−0.72	−1.81	.071	−0.83	−2.09	.037[a]	−0.73	−1.67	.095
	Age	−1.16	−3.60	<.001[b]	−1.58	−5.29	<.001[b]	−1.52	−4.72	<.001[b]
	Sex	0.22	0.34	.732	0.29	0.46	.648	0.26	0.39	.696
	ICV	0.34	1.26	.209	0.36	1.22	.224	0.32	1.09	.275
	Add: MDD until scan	–	–	–	1.42	3.13	.002[c]	1.25	2.56	.011[a]
	Add: familial risk	–	–	–	–	–	–	0.59	1.33	.183
NAA/Cr										
Left	NAA/Cr	−0.45	−1.83	.068	−0.43	−1.48	.140	−0.30	−0.92	.356
	Age	−0.98	−3.22	.001[c]	−1.31	−4.59	<.001[b]	−1.31	−4.25	<.001[b]
	Sex	−0.47	−0.65	.516	−0.61	−0.82	.414	−0.65	−0.82	.411
	Add: MDD until scan	–	–	–	1.28	2.26	.024[a]	1.06	1.78	.075
	Add: familial risk	–	–	–	–	–	–	0.85	1.74	.083
Right	NAA/Cr	−0.37	−1.63	.102	−0.30	−1.14	.253	−0.16	−0.55	.586
	Age	−0.92	−3.13	.002[c]	−1.22	−4.61	<.001[b]	−1.23	−4.08	<.001[b]
	Sex	−0.36	−0.53	.594	−0.45	−0.64	.525	−0.49	−0.64	.522
	Add: MDD until scan	–	–	–	1.17	2.06	.039[a]	0.94	1.55	.121
	Add: familial risk	–	–	–	–	–	–	0.92	1.99	.047[a]
Valence										
Left	Valence	−0.30	−0.85	.397	−0.30	−1.06	.288	−0.21	−0.68	.494
	Age	−0.87	−3.32	.001[c]	−1.10	−4.25	<.001[b]	−1.09	−3.92	<.001[b]
	Sex	−0.07	−0.13	.900	−0.16	−0.26	.796	−0.07	−0.11	.913
	Add: MDD until scan	–	–	–	1.07	2.77	.006[c]	0.91	2.07	.039[a]
	Add: familial risk	–	–	–	–	–	–	0.69	1.37	.171
Right	Valence	−0.17	−0.59	.558	−0.20	−0.77	.440	−0.10	−0.33	.739
	Age	−0.86	−3.33	.001[c]	−1.09	−4.24	<.001[b]	−1.08	−3.93	<.001[b]
	Sex	−0.06	−0.10	.924	−0.14	−0.23	.815	−0.04	−0.06	.954
	Add: MDD until scan	–	–	–	1.06	2.81	.005[c]	0.89	2.00	.046[a]
	Add: familial risk	–	–	–	–	–	–	0.73	1.37	.170
Arousal										
Left	Arousal	−0.53	−2.59	.009[c]	−0.62	−2.60	.009[c]	−0.59	−2.71	.007[c]
	Age	−0.81	−3.08	.002[c]	−1.05	−4.14	<.001[b]	−1.03	−3.96	<.001[b]
	Sex	0.08	0.13	.900	0.06	0.09	.926	0.12	0.18	.853
	Add: MDD until scan	–	–	–	1.19	2.53	.011[a]	0.99	2.22	.027[a]
	Add: familial risk	–	–	–	–	–	–	0.79	1.66	.097
Right	Arousal	−0.19	−0.87	.383	−0.23	−0.96	.335	−0.19	−0.83	.408
	Age	−0.82	−3.24	.001[c]	−1.03	−4.25	<.001[b]	−1.04	−3.95	<.001[b]
	Sex	0.00	0.00	>.99	−0.06	−0.10	.921	0.01	0.01	.988
	Add: MDD until scan	–	–	–	1.05	2.93	.003[c]	0.89	2.37	.018[a]
	Add: familial risk	–	–	–	–	–	–	0.76	1.66	.097

ICV, intracranial volume; MDD, major depressive disorder; NAA/Cr, *N*-acetylaspartate/creatine ratio.
[a] $p < .05$.
[b] $p < .001$.
[c] $p < .01$.

assay them. This has implications for study design: studies aiming to bridge across multiple brain measures should be cognizant of age, as models may not converge if the hypothesized effects are peaking at different age ranges across different brain measures.

Finally, we observed that lower putamen volume predicted episodes of MDD up to 8 years after scan. When stratified by age group, this finding was observed in individuals under, but not over, age 30. This could be because putamen structural variability was greater in the younger subgroup or because a greater proportion of individuals in the 30 years and older age group had already passed the peak age for depression onset.

Strengths and Limitations

Our findings should be interpreted in the context of several limitations. First, the sample consisted primarily of individuals of European descent, as was the norm for family studies when the project began in 1982. Thus, findings may not generalize to other populations or to other forms of depression that are not familial. Second, the study is conceptualized as an in-depth characterization of one brain region; the broader role of the putamen within frontostriatal circuits, as well as that of other striatal regions such as the nucleus accumbens and caudate nuclei, which are also implicated in depressive disorders and traits (42,43), will require future study. Third, the sample size is also modest, particularly for testing interactions, and some fMRI associations may not survive the strictest corrections for multiple testing. Corresponding strengths of our research include the longitudinal phenotyping, with onset and offset dates available for each episode allowing for better temporal clinical resolution, and the availability of multiple modalities of MRI data collected during the same scan session, which minimizes variation in scanning session, coregistration, and participant clinical characteristics at the time of scan.

Conclusions

Our findings support a role for the putamen in risk for depression, demonstrating that individuals at high familial risk for MDD have impairments in both structure and function and that these anomalies are not solely a consequence of depression. Future work is needed to replicate these findings; care also needs to be taken to model the complicating effects of age, as findings observed using different brain modalities may peak at different ages.

ACKNOWLEDGMENTS AND DISCLOSURES

This project was supported by the National Institute of Mental Health (Grant No. R01MH036197 [to MMW and JP]). The content is solely the responsibility of the authors and does not necessarily represent the official views of the National Institutes of Health or of any other sponsor.

In the past 3 years, MMW has reported receiving royalties from Oxford University Press, Perseus Books Group, American Psychiatric Association Publishing, and Multi-Health Systems. JP has received funding from Takeda (formerly Shire) and Aevi Genomics and was on an advisory board for Innovation Sciences. None of these present any conflict with the present work. All other authors report no biomedical financial interests or potential conflicts of interest.

ARTICLE INFORMATION

From the Department of Psychiatry (AT, MTvD, LP, XH, ZW, MG, ZD, JK, PJW, MMW), Columbia University Irving Medical Center and Vagelos College of Physicians and Surgeons; Division of Translational Epidemiology (AT, MTvD, LP, XH, MG, JK, PJW, MMW), Division of Translational Imaging (ZW), and Division of Molecular Imaging and Neuropathology (ZD), New York State Psychiatric Institute; and Department of Biostatistics (PJW) and Department of Epidemiology (MMW), Columbia University Mailman School of Public Health, New York, New York; Department of Psychiatry and Behavioral Sciences (SS), Northwestern University, Chicago, Illinois; and Department of Psychiatry (JP), Duke University, Durham, North Carolina.

Address correspondence to Ardesheer Talati, Ph.D., at adi.talati@nyspi.columbia.edu.

Received Jan 11, 2022; revised Jun 14, 2022; accepted Jun 16, 2022.

Supplementary material cited in this article is available online at https://doi.org/10.1016/j.biopsych.2022.06.035.

REFERENCES

1. Bolton JM, Pagura J, Enns MW, Grant B, Sareen J (2010): A population-based longitudinal study of risk factors for suicide attempts in major depressive disorder. J Psychiatr Res 44:817–826.
2. Rhee TG, Steffens DC (2020): Major depressive disorder and impaired health-related quality of life among US older adults. Int J Geriatr Psychiatry 35:1189–1197.
3. Rasic D, Hajek T, Alda M, Uher R (2014): Risk of mental illness in offspring of parents with schizophrenia, bipolar disorder, and major depressive disorder: A meta-analysis of family high-risk studies. Schizophr Bull 40:28–38.
4. Sullivan PF, Neale MC, Kendler KS (2000): Genetic epidemiology of major depression: Review and meta-analysis. Am J Psychiatry 157:1552–1562.
5. Pizzagalli DA (2014): Depression, stress, and anhedonia: Toward a synthesis and integrated model. Annu Rev Clin Psychol 10:393–423.
6. Kempton MJ, Salvador Z, Munafò MR, Geddes JR, Simmons A, Frangou S, Williams SC (2011): Structural neuroimaging studies in major depressive disorder. Meta-analysis and comparison with bipolar disorder. Arch Gen Psychiatry 68:675–690.
7. Koolschijn PC, van Haren NE, Lensvelt-Mulders GJ, Hulshoff Pol HE, Kahn RS (2009): Brain volume abnormalities in major depressive disorder: A meta-analysis of magnetic resonance imaging studies. Hum Brain Mapp 30:3719–3735.
8. Baumann B, Danos P, Krell D, Diekmann S, Leschinger A, Stauch R, *et al.* (1999): Reduced volume of limbic system-affiliated basal ganglia in mood disorders: Preliminary data from a postmortem study. J Neuropsychiatry Clin Neurosci 11:71–78.
9. Auerbach RP, Pisoni A, Bondy E, Kumar P, Stewart JG, Yendiki A, Pizzagalli DA (2017): Neuroanatomical prediction of anhedonia in adolescents. Neuropsychopharmacology 42:2087–2095.
10. Jing B, Liu CH, Ma X, Yan HG, Zhuo ZZ, Zhang Y, *et al.* (2013): Difference in amplitude of low-frequency fluctuation between currently depressed and remitted females with major depressive disorder. Brain Res 1540:74–83.
11. Surguladze S, Brammer MJ, Keedwell P, Giampietro V, Young AW, Travis MJ, *et al.* (2005): A differential pattern of neural response toward sad versus happy facial expressions in major depressive disorder. Biol Psychiatry 57:201–209.
12. Pagliaccio D, Alqueza KL, Marsh R, Auerbach RP (2020): Brain volume abnormalities in youth at high risk for depression: Adolescent brain and cognitive development study. J Am Acad Child Adolesc Psychiatry 59:1178–1188.
13. Insel T, Cuthbert B, Garvey M, Heinssen R, Pine DS, Quinn K, *et al.* (2010): Research domain criteria (RDoC): Toward a new classification framework for research on mental disorders. Am J Psychiatry 167:748–751.
14. Shankman SA, Gorka SM (2015): Psychopathology research in the RDoC era: Unanswered questions and the importance of the psychophysiological unit of analysis. Int J Psychophysiol 98:330–337.

15. Duyn JH, Gillen J, Sobering G, van Zijl PC, Moonen CT (1993): Multisection proton MR spectroscopic imaging of the brain. Radiology 188:277–282.
16. Weissman MM, Berry OO, Warner V, Gameroff MJ, Skipper J, Talati A, *et al.* (2016): A 30-year study of 3 generations at high risk and low risk for depression. JAMA Psychiatry 73:970–977.
17. Weissman MM, Wickramaratne P, Gameroff MJ, Warner V, Pilowsky D, Kohad RG, *et al.* (2016): Offspring of depressed parents: 30 years later. Am J Psychiatry 173:1024–1032.
18. Weissman MM, Wickramaratne P, Nomura Y, Warner V, Pilowsky D, Verdeli H (2006): Offspring of depressed parents: 20 years later. Am J Psychiatry 163:1001–1008.
19. van Dijk MT, Murphy E, Posner JE, Talati A, Weissman MM (2021): Association of multigenerational family history of depression with lifetime depressive and other psychiatric disorders in children: Results from the adolescent brain cognitive development (ABCD) study. JAMA Psychiatry 78:778–787.
20. Weissman MM, Wickramaratne P, Nomura Y, Warner V, Verdeli H, Pilowsky DJ, *et al.* (2005): Families at high and low risk for depression: A 3-generation study. Arch Gen Psychiatry 62:29–36.
21. Schuff N, Meyerhoff DJ, Mueller S, Chao L, Sacrey DT, Laxer K, Weiner MW (2006): N-acetylaspartate as a marker of neuronal injury in neurodegenerative disease. Adv Exp Med Biol 576:241–262; discussion 361–363.
22. Mannuzza S, Fyer AJ, Klein DF, Endicott J (1986): Schedule for Affective Disorders and Schizophrenia—Lifetime Version modified for the study of anxiety disorders (SADS-LA): Rationale and conceptual development. J Psychiatr Res 20:317–325.
23. Kaufman J, Birmaher B, Brent D, Rao U, Flynn C, Moreci P, *et al.* (1997): Schedule for Affective Disorders and Schizophrenia for School-Age Children-Present and Lifetime Version (K-SADS-PL): Initial reliability and validity data. J Am Acad Child Adolesc Psychiatry 36:980–988.
24. Leckman JF, Sholomskas D, Thompson WD, Belanger A, Weissman MM (1982): Best estimate of lifetime psychiatric diagnosis: A methodological study. Arch Gen Psychiatry 39:879–883.
25. Weissman MM, Talati A, Gameroff MJ, Pan L, Skipper J, Posner JE, Wickramaratne PJ (2021): Enduring problems in the offspring of depressed parents followed up to 38 years. EClinicalmedicine 38: 101000.
26. Tottenham N, Weissman MM, Wang Z, Warner V, Gameroff MJ, Semanek DP, *et al.* (2021): Depression risk is associated with weakened synchrony between the amygdala and experienced emotion. Biol Psychiatry Cogn Neurosci Neuroimaging 6:343–351.
27. Dong Z, Peterson B (2007): The rapid and automatic combination of proton MRSI data using multi-channel coils without water suppression. Magn Reson Imaging 25:1148–1154.
28. Hao X, Xu D, Bansal R, Dong Z, Liu J, Wang Z, *et al.* (2013): Multimodal magnetic resonance imaging: The coordinated use of multiple, mutually informative probes to understand brain structure and function. Hum Brain Mapp 34:253–271.
29. Abedelahi A, Hasanzadeh H, Hadizadeh H, Joghataie MT (2013): Morphometric and volumetric study of caudate and putamen nuclei in normal individuals by MRI: Effect of normal aging, gender and hemispheric differences. Pol J Radiol 78:7–14.
30. McDonald WM, Husain M, Doraiswamy PM, Figiel G, Boyko O, Krishnan KR (1991): A magnetic resonance image study of age-related changes in human putamen nuclei. NeuroReport 2:57–60.
31. Holmans P, Weissman MM, Zubenko GS, Scheftner WA, Crowe RR, Depaulo JR, *et al.* (2007): Genetics of recurrent early-onset major depression (GenRED): Final genome scan report. Am J Psychiatry 164:248–258.
32. Auerbach RP, Pagliaccio D, Pizzagalli DA (2019): Toward an improved understanding of anhedonia. JAMA Psychiatry 76:571–573.
33. Schaub AC, Kirschner M, Schweinfurth N, Mählmann L, Kettelhack C, Engeli EE, *et al.* (2021): Neural mapping of anhedonia across psychiatric diagnoses: A transdiagnostic neuroimaging analysis. NeuroImage Clin 32:102825.
34. Colibazzi T, Posner J, Wang Z, Gorman D, Gerber A, Yu S, *et al.* (2010): Neural systems subserving valence and arousal during the experience of induced emotions. Emotion 10:377–389.
35. Lane RD, Chua PM, Dolan RJ (1999): Common effects of emotional valence, arousal and attention on neural activation during visual processing of pictures. Neuropsychologia 37:989–997.
36. Lewis PA, Critchley HD, Rotshtein P, Dolan RJ (2007): Neural correlates of processing valence and arousal in affective words. Cereb Cortex 17:742–748.
37. Duckworth AL, Kern ML (2011): A meta-analysis of the convergent validity of self-control measures. J Res Pers 45:259–268.
38. Eisenberg IW, Bissett PG, Zeynep Enkavi A, Li J, MacKinnon DP, Marsch LA, Poldrack RA (2019): Uncovering the structure of self-regulation through data-driven ontology discovery. Nat Commun 10:2319.
39. Peng Y, Knotts JD, Taylor CT, Craske MG, Stein MB, Bookheimer S, *et al.* (2021): Failure to identify robust latent variables of positive or negative valence processing across units of analysis. Biol Psychiatry Cogn Neurosci Neuroimaging 6:518–526.
40. Shengli C, Yingli Z, Zheng G, Shiwei L, Ziyun X, Han F, *et al.* (2022): An aberrant hippocampal subregional network, rather than structure, characterizes major depressive disorder. J Affect Disord 302:123–130.
41. Dima D, Modabbernia A, Papachristou E, Doucet GE, Agartz I, Aghajani M, *et al.* (2022): Subcortical volumes across the lifespan: Data from 18,605 healthy individuals aged 3–90 years. Hum Brain Mapp 43:452–469.
42. Harvey PO, Pruessner J, Czechowska Y, Lepage M (2007): Individual differences in trait anhedonia: A structural and functional magnetic resonance imaging study in non-clinical subjects. Mol Psychiatry. 12: 12(8):703, 67–75.
43. Pizzagalli DA, Holmes AJ, Dillon DG, Goetz EL, Birk JL, Bogdan R, *et al.* (2009): Reduced caudate and nucleus accumbens response to rewards in unmedicated individuals with major depressive disorder. Am J Psychiatry 166:702–710.